76. An Analysis of the Bonding Properties of Benz[*a*]azulene by X-Ray, NMR, and Computational Studies

by **Michael Bühl, Wiktor Koźmiński, Anthony Linden, Daniel Nanz, David Sperandio**[1]), and **Hans-Jürgen Hansen***

Organisch-chemisches Institut der Universität, Winterthurerstrasse 190, CH-8057 Zürich

Dedicated to *Edgar Heilbronner* on the occasion of his 75th birthday

(1.II.96)

The X-ray crystal structures of 9-phenylbenz[*a*]azulene (**4**) and the corresponding non-benzannelated form, 4-phenylazulene (**5**), have been determined (*cf. Fig. 2*). In contrast to **5**, the skeleton of which shows nearly equal C,C bond lengths (*cf. Table 1*), the seven-membered ring of **4** exhibits clearly alternating C,C bond lengths (*cf. Table 1*). This is in agreement with a strong accentuation of the heptafulvene substructure in **4** by the [*a*] benzannelation. The alternating bond lengths of **4** and of its parent structure **3** are also reflected in the corresponding variations of the ^3J(H,H) and $^1J(^{13}C,^{13}C)$ values of these benz[*a*]azulenes (*cf. Tables 4* and *5*). Computations on the MP2/6-31G* level as well as on the BP86/6-31G* level for azulene (**6**), benz[*a*]azulene (**3**), and heptafulvene (**7**) are in good agreement with the experimental values (*cf. Tables 6–8*).

1. Introduction[2]). – Recently, we have published a new synthesis of benz[*a*]azulene (**3**) [1], based on the intramolecular *Heck* reaction of a suitably substituted heptafulvene **1** (*cf. Scheme 1*). The intermediate, 10-(phenylsulfonyl)benz[*a*]azulene (**2**), formed in the first step, could also be used for the selective introduction of substituents, *e.g.* a Ph group, at C(9) of the benz[*a*]azulene skeleton (*cf. Scheme 1*).

Scheme 1

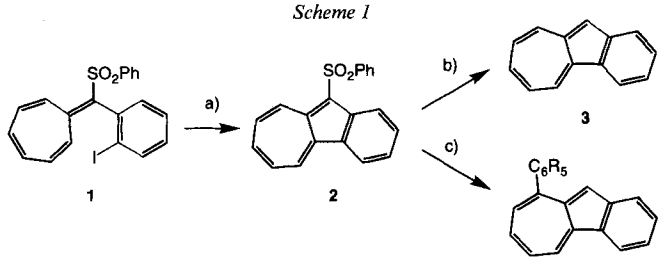

a) 0.5 mol-% $Pd(OAc)_2$, $Bu_4N^+Cl^-$, $NaHCO_3$ / DMF, room temp. / 30 h; 92%. b) $Na_2S_2O_4$, $NaHCO_3$ / DMF + H_2O, 85–90° / 17 min; 78%. c) 1. PhLi ((D_5)PhLi) / THF, −78°; 2. 3,4,5,6-tetrachloro-1,2-benzoquinone (*o*-chloroanil) / toluene, room temp.; 70%. 3. $Na_2S_2O_4$, $NaHCO_3$ / DMF + H_2O, 85–90° / 20 min; 72%.

[1]) Part of the planned Ph. D. thesis of *D. S.*, University of Zurich, 1996.

[2]) We also wish to celebrate, on this occasion, the '60th anniversary' of the work of *Pfau* and *Plattner* on the correct structure of azulenes which appeared in this journal [1a].

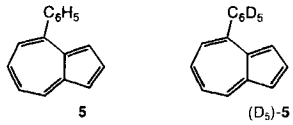

5 (D5)-5

Inconsistencies between some ^{1}H chemical-shift assignments for **3** (*cf.* [1b]) and those published by *Bertelli* and *Crews* [2], as well as a peculiarity in the ^{1}H-NMR spectrum of **3** in $CDCl_3$ (see later), led us to study the bonding situation in **3** and its 9-Ph derivative **4** in more detail. For ^{1}H-NMR measurements, we also prepared the deuterated benz[*a*]-azulene (D_5)-**4** (*cf. Scheme 1*). To gain more insight into the degree to which the [*a*] benzannelation influences the azulene structure in terms of an accentuation of the inherent heptafulvene substructure (*cf.* also [2]), we also included 4-phenylazulene (**5**) in our investigations.

Compound **5** had already been prepared and reported as a blue oil [3]. Fortunately, carefully purified **5** crystallized from hexane as blue prisms (m.p. 34–35°; see *Exper. Part*). This allowed us to study the X-ray crystal structures of **5** and, for comparison, its [*a*] benzannelated analogue **4**.

2. X-Ray Crystal-Structure Analyses. – The *Cambridge Structural Database* (CSD) [4] contains many X-ray crystal structures of azulenes. Of these, there are 23 examples with a simple substitution pattern in which the substituents are not expected to have a significant effect on the electronic nature of the azulene core [5]. Each of these structures shows almost no variation in the bond lengths around the perimeter of the azulene ring system. These bond lengths are consistent with those expected for a completely delocalized aromatic carbon π-system. On the other hand, the central C(3a),C(8a) bond lengths are more representative of pure C–C bonds. *Fig. 1* illustrates four examples of these structural features.

In contrast, theoretical calculations on the structure of **3** (see *Chapt. 4*) as well as the variation in the ^3J(H,H) values of **3** [2] (see also the following section) indicate that the

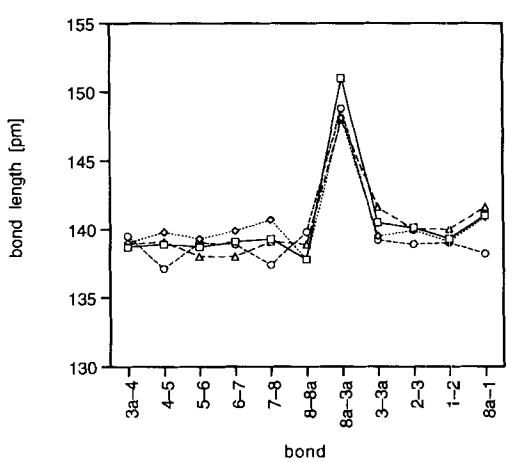

Fig. 1. *Bond lengths of simply substituted azulenes, depicted using four representative examples* (in parentheses CSD refcodes [5]). —□—: [2.2](1,3)Azulenophane (azulop); ···◇···: [2](5,7)Azuleno[2]paracyclophane (besvaw); ---○---: 4,6,8-Trimethylazulene (damhee); ---△---: (*E,E*)-1,3-Di(phenylethenyl)azulene (styraz).

π-system of the azulene core of **3** is perturbed by the [*a*] benzannelation in such a way that the underlying heptafulvene structure is more pronounced. As a result, the alternating pattern of C–C and C=C bonds becomes more evident. A search of the *CSD* revealed that no X-ray crystal-structure determinations of benz[*a*]azulenes have been reported, and thus the extent of the variations in these compounds could not be verified[3]).

Therefore, we attempted to determine the solid-state structure of unsubstituted benz[*a*]azulene (**3**). Well-formed crystals of **3** could be grown from hexane, and two independent sets of X-ray diffraction data were recorded using different crystals. In each case, reflection profiles showed no evidence for inferior crystal quality. However, attempts to refine the structure revealed that the molecules are either highly disordered, or that the crystals are twinned. These difficulties could not be resolved satisfactorily, and it was not possible to draw conclusions regarding the bonding within the molecule.

As an alternative, we investigated the structure of 9-phenylbenz[*a*]azulene (**4**). Here, the structure determination was successful and produced accurate structural parameters (*cf. Fig. 2*). The crystals of **4** contain two independent molecules in the asymmetric unit. However, there are no significant differences between their geometries.

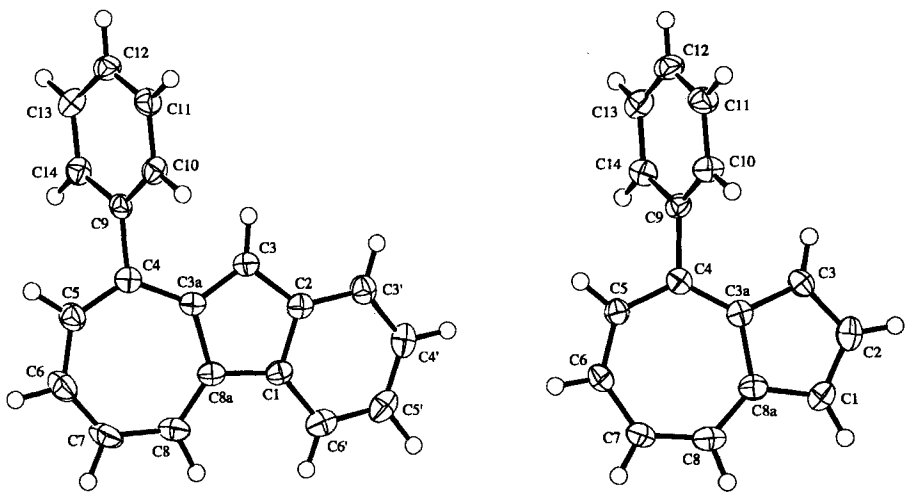

Fig. 2. *X-Ray crystal structures of 9-phenylbenz[a]azulene* (**4**) *and 4-phenylazulene* (**5**)

For a direct comparison of the effect of the benzannelation on the structure of the azulene core as well as to account for the possible influence of the Ph substituent, we also determined the solid-state structure of 4-phenylazulene (**5**; see *Fig. 2* and *Table 1*). The bond lengths for the azulene core of **4** and **5** are given in *Table 1*.

When the estimated standard deviations (e.s.d.) are taken into account, the maximum difference between any two of the bond lengths of **5** is insignificant. These bonds can, therefore, be considered to be equivalent, which means that the carbon π-system of **5** is almost completely delocalized, as expected. In contrast, the structure of **4** shows a

[3]) According to the *CSD*, only one X-ray crystal structure of a benzazulene, namely that of 10-(methylamino)benz[*f*]azulene, has been determined [6].

Table 1. *Bond Lengths* [pm] (e.s.d. in parentheses) *of 9-Phenylbenz[a]azulene* (**4**) *and 4-Phenylazulene* (**5**) *According to the X-Ray Crystal-Structure Analyses*

Bond[a])	**4**[b])	**5**	Bond	**4**[b])	**5**
C(1)–C(2)	141.7(3)	138.7(4)	C(4)–C(5)	137.3(3)	141.2(4)
C(1)–C(8a)	145.4(3)	140.2(4)	C(5)–C(6)	142.6(3)	137.9(4)
C(1)–C(6′)	140.3(3)	–	C(6)–C(7)	136.0(3)	138.5(4)
C(2)–C(3)	143.9(3)	139.7(4)	C(7)–C(8)	142.2(3)	140.0(4)
C(2)–C(3′)	140.4(3)	–	C(8)–C(8a)	136.1(3)	137.6(4)
C(3)–C(3a)	138.0(3)	140.4(4)	C(3′)–C(4′)	138.6(3)	–
C(3a)–C(4)	143.9(3)	138.9(4)	C(4′)–C(5′)	139.9(3)	–
C(3a)–C(8a)	149.3(3)	150.8(4)	C(5′)–C(6′)	138.6(3)	–

[a]) To simplify the comparison, we use the following C-atom numbering for **4**:

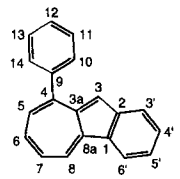

[b]) Mean values from the two independent molecules.

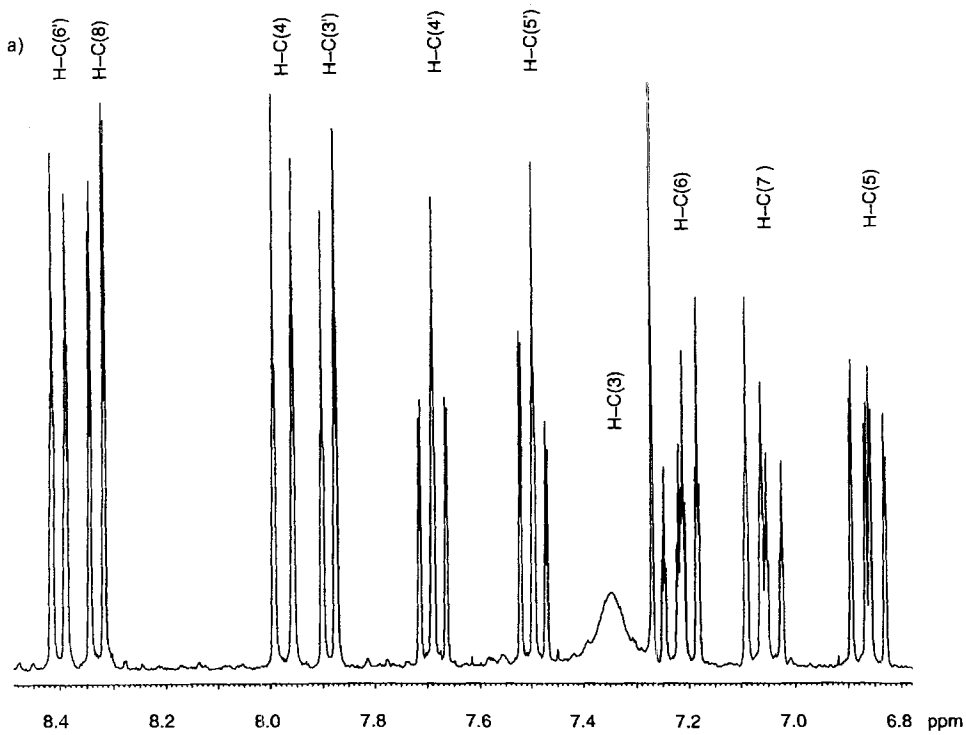

Fig. 3. a) *^{1}H-NMR Spectrum* (300 MHz) *of* **3** *in $CDCl_3$ showing the almost complete disappearance of the* singlet *of H–C(3) at 7.34 ppm.* b) *Reference ^{1}H-NMR spectrum* (600 MHz) *of* **3** *in CD_2Cl_2 with the sharp* singlet *of H–C(3) at 7.23 ppm*

distinctly alternating pattern of bond lengths around the seven-membered ring. The maximum difference between any two of these bond lengths is 7.9 pm which, when compared with the bond length e.s.d.'s, is a significant variation. This indicates that the carbon π-system of **4** is perturbed substantially, showing the tendency towards a localized heptafulvene substructure.

In both structures, the Ph substituent does not seem to influence the geometry of the azulene ring system significantly. Furthermore, the torsion angle between the plane of the Ph ring and the plane of the azulene part in **4** (58°) and **5** (69°) shows that the Ph substituent does not conjugate with the azulene π-system. Therefore, it can reasonably be assumed that these two structures are representative of those of the unsubstituted parent compounds.

3. NMR Measurements. – We recorded and fully assigned the ^{1}H- and ^{13}C-NMR spectra of benz[*a*]azulene (**3**), 9-(($^2H_5$)phenyl)benz[*a*]azulene ((D$_5$)-**4**), and its non-benz-annelated analogue (D$_5$)-**5**. To circumvent solubility problems, most of the spectra of **3** and (D$_5$)-**4** were measured in CD_2Cl_2. The ^{1}H-NMR spectra of **3** in $CDCl_3$ showed in some cases a varying and, at first, incomprehensible line broadening of the *singlet* of H–C(3)[4])

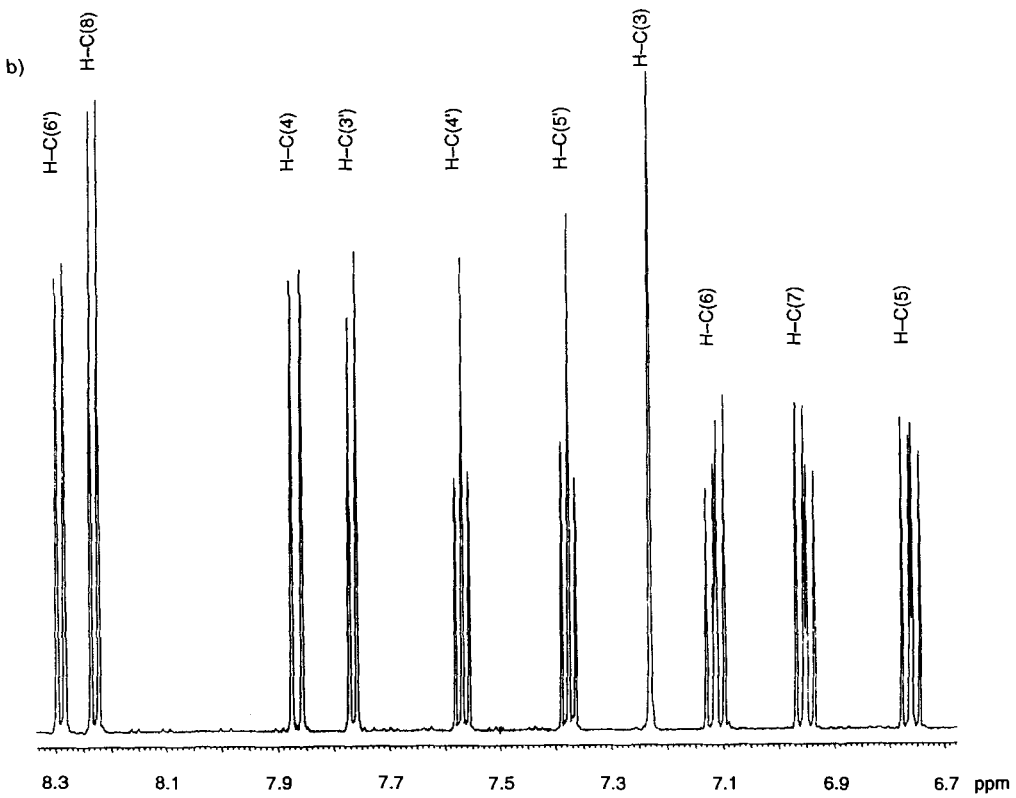

Fig. 3 (cont.)

[4]) See Footnote *a* in *Table 1* for numbering.

at 7.34 ppm, which, in the extreme, led to a complete vanishing of the signal. *Fig. 3, a*, documents this effect. It is accompanied by a disappearance of ^5J(H–C(3),H–C(8)), which amounts to 1.0 Hz in the reference spectrum in CD_2Cl_2 (*cf. Fig. 3, b*).

The other coupling patterns were not altered. The broadening of the H–C(3) signal was not observed in other solvents (CD_2Cl_2, (D_6)acetone, CS_2, CCl_4) and could also be suppressed in degassed $CDCl_3$. On the other hand, the addition of traces of a strong acid, *e.g.* HCl, to the $CDCl_3$ solution of **3** re-established the line broadening of the H–C(3) signal. Obviously, **3** is sufficiently basic to undergo a rapid proton exchange with traces of strong acids which are either present in (DCl), or added to (HCl), $CDCl_3$. We have never observed this effect with other azulenes and, indeed, as has already been shown by *Heilbronner* and coworkers [7], **3** is by far the most basic azulene derivative when compared with other benzazulenes and azulene itself.

The ^{1}H chemical shifts of **3** in different solvents are collected in *Table 2*. The ^{1}H-shift assignments for **3** are largely the same as those reported by *Bertelli* and *Crews* [2], with the exception of those for H–C(4) and H–C(3′) as well as for H–C(8) and H–C(6′), which had to be interchanged. The reassignments are corroborated by a proton-detected INEPT-INADEQUATE experiment (*cf.* [8]). The chemical shifts of the H-atoms of the azulene and the benzo moiety of **3** are only moderately influenced by the solvents (*cf. Table 2*).

Table 2. *Solvent Effects on the ^{1}H Chemical Shifts* [ppm] *of* **3**

H-Atom[a])	$CDCl_3$	CH_2Cl_2	CCl_4	CS_2	(D_6)Acetone
H–C(6′)	8.38	8.29	8.26	8.17	8.51
H–C(8)	8.30	8.23	8.20	8.13	8.49
H–C(4)	7.95	7.87	7.85	7.80	8.04
H–C(3′)	7.88	7.77	7.75	7.67	7.88
H–C(4′)	7.67	7.57	7.57	7.51	7.67
H–C(5′)	7.48	7.38	7.36	7.32	7.48
H–C(3)	7.33	7.23	7.23	7.15	7.38
H–C(6)	7.19	7.12	7.10	7.09	7.29
H–C(7)	7.04	6.95	6.95	6.92	7.13
H–C(6)	6.84	6.76	6.74	6.72	6.93

[a]) For numbering, see *Footnote a* in *Table 1*.

The solvent effect is most pronounced for the chemical shifts of H–C(8) and H–C(6′), *i.e.*, the two opposed *peri*-H atoms, which are displaced to lower frequencies as the polarity of the solvent decreases. The ^{13}C chemical shifts of the azulene **3** follow *grosso modo* the same trend as the ^{1}H chemical shifts (*cf. Table 3*).

Table 4 contains the ^3J(H,H) values of the azulenes. Whereas 4-(($^2H_5$)phenyl)azulene ((D_5)-**5**), like other simply substituted azulenes (*cf.* [9]), shows nearly equal ^3J(H,H) values for all atoms around the seven-membered ring, there is a clear variation in these values for benzo[*a*]azulenes **3** and (D_5)-**4**, which is in accordance with their accentuated heptafulvene substructure (see also [2]). The coupling constants vary between 8.5 Hz across formal C–C bonds and 11.0 Hz across formal C=C bonds. These values are close to those of heptafulvene which shows ^3J(H,H) values of 7.5 Hz and 11.5–12.0 Hz, respectively [10] (see also *Chapt. 5*).

Table 3. *Solvent Effects on the ^{13}C Chemical Shifts* [ppm] *of* **3**

C-Atom[a])	$CDCl_3$	CCl_4	CH_2Cl_2	CS_2	(D_6)Acetone
C(2)	142.40	142.27	142.36	142.21	143.44
C(8a)	140.58	140.76	140.38	140.42	141.46
C(3a)	139.20	138.74	139.16	138.68	140.17
C(4)	135.94	135.72	135.81	135.76	136.83
C(6)	134.64	133.90	134.72	134.23	135.84
C(1)	131.41	131.28	131.33	131.17	132.44
C(4′)	128.48	128.20	128.45	128.48	129.40
C(8)	127.86	126.96	127.99	127.28	129.24
C(7)	125.35	124.87	125.32	125.12	126.45
C(5)	123.66	122.93	123.72	123.41	124.82
C(5′)	121.78	121.52	121.72	121.81	122.74
C(6′)	120.78	120.41	120.74	120.57	121.91
C(3′)	120.25	120.01	120.14	120.22	121.01
C(3)	116.06	116.31	115.92	116.76	116.96

[a]) For numbering, see *Footnote a* in *Table 1*.

Table 4. *$^3J(H,H)$ Values* [Hz] *of* **3**, *(D_5)-***4**, *and (D_5)-***5**

^3J[a])	**3**	(D_5)-**4**	(D_5)-**5**
$^3J(7,8)$	8.3	8.3	9.4
$^3J(6,7)$	11.1	10.9	10.1
$^3J(5,6)$	8.5	9.0	10.1
$^3J(4,5)$	10.9	–	–
$^3J(3',4')$	7.9	7.8	–
$^3J(4',5')$	7.0	7.1	–
$^3J(5',6')$	8.0	7.9	–

[a]) For numbering, see *Footnote a* in *Table 1*.

Table 5. *$^1J(^{13}C,^{13}C)$ Values* [Hz] *of* **3** *and (D_5)-***4**

^1J	**3**	(D_5)-**4**	^1J	**3**	(D_5)-**4**
$^1J(8,8a)$	66.9	66.8	$^1J(2,3)$	55.6	55.3
$^1J(8,7)$	56.4	56.4	$^1J(2',3')$	58.6	58.6
$^1J(6,7)$	63.0	63.0	$^1J(3',4')$	58.6	58.6
$^1J(5,6)$	55.1	54.9	$^1J(4',5')$	55.9	58.4
$^1J(4,5)$	64.4	66.4	$^1J(5',6')$	58.8	58.4
$^1J(3a,4)$	58.0	–	$^1J(6',1)$	61.2	60.5
$^1J(3,3a)$	65.4	66.2			

[a]) For numbering, see *Footnote a* in *Table 1*.

The $^1J(^{13}C,^{13}C)$ values of **3** and (D_5)-**4** are collected in *Table 5*. Because of the low sample concentration even in a saturated solution of **3**, two new proton-detected experiments were developed (*cf* [11]) in order to measure these coupling constants in CD_2Cl_2. The tabulated values were obtained from proton-detected INEPT-*J*-resolved (PDIJ) experiments [11], performed with samples of 0.11 mM (**3**) and 0.065 mM ((D_5)-**4**)

in 0.5 ml CD_2Cl_2 solutions. The estimated errors of the coupling constants are *ca.* ±0.2 Hz for **3** and *ca.* ±0.5 Hz for (D_5)-**4**. The spectra of the latter compound displayed a significantly lower signal-to-noise ratio. The coupling constants of C_2 fragments that do not carry directly attached H-atoms are not detected in the described experiments.

The measured $^1J(^{13}C,^{13}C)$ values are again in excellent agreement with an accentuated heptafulvene structure in **3** and (D_5)-**4**. The average value across formal C=C bonds at the seven- and five-membered ring of **3** amounts to 64.5 ± 1.5 Hz, whereas the average value across formal C–C bonds is 56.1 ± 1.1 Hz. The corresponding values for azulene itself show nearly no variation, and their average is 58.6 ± 1.8 Hz (*cf.* [9] [12]), *i.e.*, the average $^1J(^{13}C,^{13}C)$ value for azulene lies well within the limits of the corresponding values found for **3**. The same observations were made with (D_5)-**4** (*cf. Table 5*).

4. Computational Studies. – 4.1. *Geometries.* In accordance with recent theoretical results (see *e.g.* [13]), the C_{2v}-symmetrical form of azulene (**6**) is not a minimum at the SCF/6-31G* level. In the minimized structure, **6** distorts to a planar C_s structure with largely localized C–C and C=C bonds (formal C=C bonds between 135.7 and 136.6 pm; formal C–C bonds around the perimeter between 141.8 and 142.9 pm). This form is an artifact of the SCF method, as re-optimization at both BP86/6-31G* (see also [14]) and MP2/6-31G* levels affords the C_{2v} structure with essentially equalized bonds around the perimeter (between 139.3 and 140.6 pm at MP2/6-31G*). Likewise, the SCF/6-31G* structure of benz[*a*]azulene (**3**) is too strongly localized (formal C=C bonds in the azulene fragment between 134.1 and 140.1 pm; formal C–C bonds around the perimeter between 144.3 and 146.6 pm; see *Table 6*).

A trend towards bond equalization is apparent in the electron-correlated MP2/6-31G* and PB86/6-31G* geometries, but a substantial degree of bond alternation remains around the perimeter (between 138.1 and 142.6 pm at MP2/6-31G*). A similar degree of bond alternation is apparent in the solid-state structure of 9-phenylbenz[*a*]azulene (**4**), as discussed above (*cf. Table 1*). The geometrical parameters computed at the BP86/6-31G* and MP2/6-31G* level for the parent benz[*a*]azulene (**3**) agree quite well with those determined for **4** (*cf. Table 6*).

For comparison, the structure of heptafulvene (**7**) was also calculated. At the highest level, MP2/6-31G*, the planar C_{2v}-symmetrical **7** is a true minimum. The calculated bond lengths (*cf. Table 6*) for this structure show even larger variations than those of **3**, indicating that a certain degree of delocalization is still present in **3**.

4.2. *Chemical Shifts.* As is apparent from the above theoretical results for azulene (**6**) and benz[*a*]azulene (**3**), electron-correlation effects are important for a correct description of the molecular geometry. To what extent is this also true for chemical-shift calculations in these cases? With the advent of the so-called distributed-gauge methods (for a recent review, see *e.g.* [15]), it has now become possible to routinely compute the chemical shifts of the lighter nuclei at SCF levels [16] [17], and, more recently, also at electron-correlated levels such as GIAO-MP2 [18] [19], GIAO-MP3 [20], and GIAO-CCSD [21]. It has turned out that the chemical shifts of atoms involved in multiple bonds can be quite sensitive to electron-correlation effects (*cf.* the $\delta(^{13}C)$ values computed with very large basis sets for ethylene, 135.8 (GIAO-SCF), 130.3 ppm (GIAO-MP2) [19], and 127.9 ppm (GIAO-CCSD) [21] *vs.* experiment, 130.6 ppm). To see if a comparable

Table 6. *Computed Bond Lengths* [pm] *of* **3**, **6**, *and* **7**

Bond[a])	Benz[*a*]azulene (**3**)					Azulene (**6**)					Heptafulvene (**7**)			
	MNDO	SCF	BP86	MP2	Obs.[b])	MNDO[c])	SCF[c])	BP86	MP2	Obs.[b]) [9]	SCF	BP86	MP2	Obs.[b]) [10]
C(1),C(2)	144.1	140.1	144.3	143.2	141.8	137.6	136.2	141.3	140.5	139.9	–	–	–	–
C(1),C(8a)	148.4	146.6	144.8	143.7	145.4	147.3	142.9	141.4	140.6	141.8	133.4	137.0	136.1	135.0
C(2),C(3)	140.3	145.2	143.6	142.6	143.9	145.6	142.8	141.3	140.5	139.9	–	–	–	–
C(2)C(3′)	140.3	139.2	141.5	141.1	140.4	–	–	–	–	–	–	–	–	–
C(3′),C(4′)	140.7	138.0	139.7	138.7	138.6	–	–	–	–	–	–	–	–	–
C(3),C(3a)	138.1	134.9	139.6	139.2	138.1	138.9	136.7	141.4	140.6	141.8	–	–	–	–
C(3a),C(8a)	149.8	148.6	150.0	149.1	149.3	149.9	148.5	150.7	150.3	150.1	147.4	146.9	146.3	145.0
C(4′),C(5′)	140.8	139.7	142.0	141.6	139.9	–	–	–	–	–	–	–	–	–
C(4),C(8a)	145.0	144.3	142.1	141.1	143.9	144.1	141.7	140.0	139.3	138.3	133.2	136.7	136.1	136.5
C(5′),C(6′)	140.9	138.1	139.7	138.7	138.6	–	–	–	–	–	–	–	–	–
C(5),C(4)	136.0	134.1	138.9	138.6	137.4	136.5	135.8	140.7	140.0	140.6	146.0	145.0	144.7	147.0
C(6′),C(1)	140.4	139.0	141.1	140.8	140.2	–	–	–	–	–	–	–	–	–
C(6),C(5)	144.7	144.7	142.5	141.4	142.6	136.5	142.2	140.6	140.0	140.3	133.1	136.8	136.0	133.4
C(6),C(7)	136.0	134.2	138.9	138.7	136.0	144.1	135.9	140.6	140.0	140.3	146.0	145.0	144.7	147.0
C(8),C(7)	144.8	144.5	142.6	141.4	142.3	144.1	142.0	140.7	140.0	140.6	133.2	136.7	136.1	136.5
C(8),C(8a)	136.2	134.1	138.3	138.1	136.2	136.6	135.8	140.0	139.3	138.3	147.4	146.9	146.3	145.0

[a]) For numbering, see *Footnote a* in *Table 1*.

[b]) This work; *cf. Table 1*.

[c]) False C_s-symmetrical minimum.

accuracy can be achieved for azulenes, we have computed the chemical shifts of the parent azulene (**6**) and of benz[*a*]azulene (**3**) at the GIAO-SCF/tzp level employing various sets of geometries. In addition, the ^{13}C chemical shifts of **6** have been computed at the electron-correlated GIAO-MP2/TZP′//MP2/6-31G* level. The results are summarized in *Tables 7* and *8*.

The geometry dependence of the $\delta(^{13}C)$ GIAO-SCF/tzp data for azulene (**6**) is not very pronounced. Typically, differences of only a few ppm are found between the results for the SCF, BP86, and MP2/6-31G* geometries. The overall performance in terms of the (weighted) mean absolute deviations from experiment is quite similar for these sets of geometries, namely 3.1, 4.7, and 4.3 ppm, respectively. A comparison of the GIAO-SCF/tzp and GIAP-MP2/TZP′//MP2/6-31G* results reveals notable electron-correlation effects on the computed ^{13}C chemical shifts, up to *ca.* 10 ppm (*Table 7*). The ionic character of the C_{2v} structure appears to be overestimated at the SCF-level (*cf.* for instance the C(1,3) resonance, which is computed to be too strongly shielded at GIAO-SCF/tzp// MP2/6-31G* (112.2 ppm *vs.* experimental 118.1 ppm), or the C(6) resonance, which is computed to be too strongly deshielded (142.4 ppm *vs.* experimental 137.1 ppm)). Thus, the computed chemical shifts are in line with the fact that the dipole moment is computed to be too large at SCF levels [13] (*e.g.* 1.520 D at SCF/6-31G*; *cf.* the experimental gas-phase value of 0.79 ± 0.01 D [22]). Inclusion of electron correlation reduces the ionic character (*cf.* the MP2/6-31G* dipole moment of 1.008 D), and, thus, the separation of the theorectical C(1,3) and C(6) resonances (GIAO-MP2: 117.2 and 134.2 ppm, experimental 118.1 and 137.1 ppm, respectively). As has been observed in other cases [19], the GIAO-SCF results tend to be 'overcorrected' at the GIAO-MP2/TZP′ level, *i.e.*, the deviations from experiment are of similar magnitude, but in opposite directions for the GIAO-SCF and GIAO-MP2 data. Hence, the performance of the GIAO-MP2/TZP′ results in terms of the mean abolute deviation, 3.3 ppm, is only slightly improved compared with that of the corresponding GIAO-SCF/tzp data, 4.3 ppm. More accurate theoretical results would probably require even larger basis sets and/or higher levels of electron correlation in the chemical-shift calculations [20] [21].

Unfortunately, benz[*a*]azulene (**3**) is currently too large for a GIAO-MP2/TZP′ calculation. Mean absolute deviations from experiment for the GIAO-SCF/tzp $\delta(^{13}C)$ values in *Table 7* are 1.2, 2.7, and 3.0 ppm, when the SCF, BP86, and MP2/6-31G* geometries, respectively, are employed, *i.e.*, comparable to the corresponding data for azulene (**6**). The very good performance of the SCF/6-31G* geometry is probably somewhat fortuitous. Even though the sequence of some close-lying signals is not correctly reproduced at the theoretical levels employed, the *ab initio* data have been helpful in identifying possible errors in the first, tentative assignments, which were confirmed, as mentioned above, by a proton-detected INEPT-INADEQUATE experiment.

As ^{1}H chemical shifts are a sensitive probe of ring-current effects in aromatic compounds, theoretical ^{1}H magnetic shieldings of benzene and related compounds have been studied in great detail (see *e.g.* [23]). The ^{1}H chemical shifts computed for azulene (**6**), benz[*a*]azulene (**3**), and heptafulvene (**7**) are summarized in *Table 8*. Interestingly, the GIAO-SCF/tzp $\delta(^{1}H)$ values are shifted to higher frequency by *ca.* 0.4–0.5 ppm in going from the more 'localized' SCF/6-31G* geometries to the more 'C,C-bonded equalized' BP86 and MP2/6-31G* geometries. This is consistent with a higher degree of cyclic delocalization and, thus, with greater aromaticity in the latter. The overall agreement of

Table 7. *^{13}C Chemical Shifts* [ppm] *of* **3**, **6**, *and* 7

C-Atom[a])	Benz[*a*]azulene (**3**)				Azulene (**6**)				Heptafulvene (**7**)			
	SCF	BP86	MP2	Obs.[b])	SCF[c])	BP86	MP2	Obs.[b]) [9]	SCF	BP86	MP2	Obs.[b]) [10]
C(1)	131.3	128.3	127.7	131.41	114.6	111.8	112.2	118.1	–	–	–	–
C(2)	142.5	143.0	142.8	142.40	134.4	135.5	136.2	136.9	–	–	–	–
C(3)	115.7	108.9	108.8	116.06	114.6	111.8	112.2	118.1	108.1	106.5	107.4	111.9
C(3′)	119.1	118.1	118.9	120.25	–	–	–	–	–	–	–	–
C(3a)	137.6	138.4	138.5	139.20	137.1	135.9	136.7	140.2	146.2	148.0	148.5	146.6
C(4)	134.2	139.6	141.2	135.94	139.1	141.4	141.6	136.4	135.8	137.9	138.7	138.3
C(4′)	128.8	129.3	129.6	128.48	–	–	–	–	–	–	–	–
C(5)	121.3	121.0	121.5	123.66	119.0	118.2	118.7	122.6	124.0	125.3	125.6	126.9
C(5′)	121.4	119.1	119.4	121.78	–	–	–	–	–	–	–	–
C(6)	132.9	138.0	139.1	134.64	139.8	142.6	142.4	137.1	128.3	130.4	130.8	130.8
C(6′)	121.5	122.5	123.0	120.78	–	–	–	–	–	–	–	–
C(7)	123.5	122.8	123.1	125.35	119.0	118.2	118.7	122.6	128.3	130.4	130.8	130.8
C(8)	125.7	129.9	131.6	127.86	139.1	141.4	141.6	136.4	124.0	125.3	125.6	126.9
C(8a)	138.8	135.8	136.4	140.58	137.1	135.9	136.7	140.2	135.8	137.9	138.7	138.3

[a]) For numbering, see *Footnote a* in *Table 1*. [b]) In $CDCl_3$. [c]) Average values for the false C_s minimum.

Table 8. *^{1}H Chemical Shifts* [ppm] *of* **3**, **6**, *and* **7**

H-Atom[a])	Benz[*a*]azulene (**3**)				Azulene (**6**)				Heptafulvene (**7**)			
	//SCF	//BP86	//MP2	Obs.[b])	//SCF[c])	//BP86	//MP2	Obs.[b]) [9]	//SCF	//BP86	//MP2	Obs.[b]) [10]
H–C(2)	–	–	–	–	7.6	7.9	8.0	7.82	–	–	–	–
H–C(3)	7.0	7.4	7.5	7.33	7.2	7.4	7.5	7.33	4.3	4.3	4.3	4.45
H–C(3′)	7.6	7.8	7.9	7.88	–	–	–	–	–	–	–	–
H–C(4)	7.4	8.2	8.3	7.95	8.0	8.5	8.6	8.26	5.7	5.8	5.9	5.97
H–C(4′)	7.5	7.7	7.7	7.67	–	–	–	–	–	–	–	–
H–C(5)	6.3	6.8	6.9	6.84	6.8	7.0	7.1	7.13	5.1	5.1	5.1	5.48
H–C(5′)	7.3	7.4	7.4	7.48	–	–	–	–	–	–	–	–
H–C(6)	7.4	7.5	7.2	7.19	7.5	7.9	7.9	7.51	5.2	5.3	5.3	5.65
H–C(6′)	8.2	8.6	8.7	8.38	–	–	–	–	5.7	5.8	5.9	5.97
H–C(7)	6.5	7.0	7.1	7.04	6.8	7.0	7.1	7.13	5.2	5.3	5.3	5.65
H–C(8)	7.6	8.5	8.7	8.30	8.0	8.5	8.6	8.26	5.1	5.1	5.1	5.48

[a]) For numbering, see *Footnote a* in *Table 1*. [b]) In $CDCl_3$. [c]) Average values for the false C_s minimum.

experimental and computed ^{1}H chemical shifts is quite good, with mean absolute deviations for the SCF, BP86, and MP2/6-31G* geometries of 0.2, 0.2, 0.2 ppm (**6**), and 0.4, 0.1, 0.2 ppm (**3**), and 0.4, 0.3, 0.2 ppm (**7**), respectively.

The computed ^{13}C chemical shifts for heptafulvene (**7**) are in very good agreement with the experimental values [24]. The largest deviation, 4.5 ppm, is found for the chemical shift of the methylene C-atom. The tentative assignments for the chemical shifts of C(5,8) and C(6,7)[4]) (= C(2,5) and C(3,4)) in [24] are fully supported by our theoretical results.

5. Concluding Remarks. – The experimental as well as the computational results that have been presented in the preceding sections are in accordance with the view that benz[*a*]azulenes are best described as *o*-phenylene 1,8-bridged heptafulvenes, as has been already proposed by *Bertelli* and *Crews* [2]. However, our X-ray crystal-structure analyses of **4** and **5** show quantitatively for the first time the extent of bond-length alternation in **4** compared with the relatively equivalent bond lengths in **5** which is a typical, simply substituted azulene. *Fig. 4* shows the variation of the bond lengths in **4** and **5** compared with those in azulene (**6**) [9], which represents the aromatic bonding extreme, and heptafulvene (**7**), which portrays the non-aromatic bonding extreme [10]. *Fig. 4* clearly

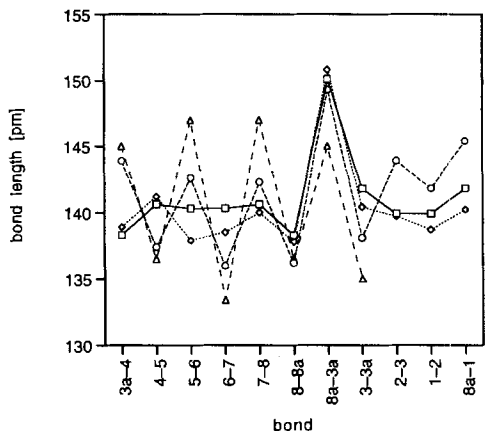

Fig. 4. *Bond-length variation* [pm] *in 4-phenylbenz[*a*]azulene* (**4**), *4-phenylazulene* (**5**), *azulene* (**6**) [9], *and heptafulvene* (**7**) [10] (for numbering, see *Footnote a* in Table 1).
---○---: **4**; ····◇····: **5**; ——□——: **6**; ---△---: **7**.

demonstrates that the bond-length alternation in **7** is also reflected in the bond distances in **5**, albeit to a much smaller extent. On the other hand, there is nearly no variation in the bond lengths of **6**, and the small unsystematic alternations in the bond lengths around the seven-membered ring of **5** can be attributed to the Ph substituent at C(4). Moreover, the computed bond lengths of benz[*a*]azulene (**3**) itself, whose X-ray crystal structure we were unable to resolve satisfactorily, are in full agreement with those observed for **4** (*cf. Table 6*).

Further information about the bonding situation of benz[*a*]azulenes comes from the ^3J(H,H) values for the seven-membered rings of **3** and **5**. Their ^3J(H,H) values show, in contrast to those of azulenes, significant alternation between 11.0 ± 0.1 Hz across formal C=C bonds and 8.5 ± 0.3 Hz across formal C–C bonds (see also [2]). The corresponding ^3J(H,H) values of simple azulenes, 9.8 ± 0.4 Hz, fall well within the range of those of **3** and **4**. The larger ^3J(H,H) values across the C=C bonds of **7** (11.5–12.1 Hz [24]) and of perfectly planar cycloheptatrienes (11.8–12.6 Hz; *cf.* [25]) point again to the fact that a localized heptafulvene substructure is not fully developed in benz[*a*]azulenes, *i.e.*, there is still a certain degree of azulene conjugation recognizable in **3**, **4**, and their derivatives. The magnitude of the measured $^1J(^{13}C,^{13}C)$ values of **3** and (D_5)-**4** fully supports this view (*cf. Table 5*).

That the azulene character of the benz[*a*]azulenes is still important can also be derived from their cycloaddition chemistry (*cf.* [26–28]). In the thermal reaction with dimethyl acetylenedicarboxylate (ADM), they form, in analogy to azulenes, the corresponding dimethyl benzo[*a*]heptalene-6,7-dicarboxylates **11** *via* benzannelated tricyclo[6.2.2.$0^{1,7}$]-dodeca-2,4,6,9,11-pentaene-9,10-dicarboxylates **10**, which are created in the primary addition step (*Scheme 2*; see also [25]).

Scheme 2

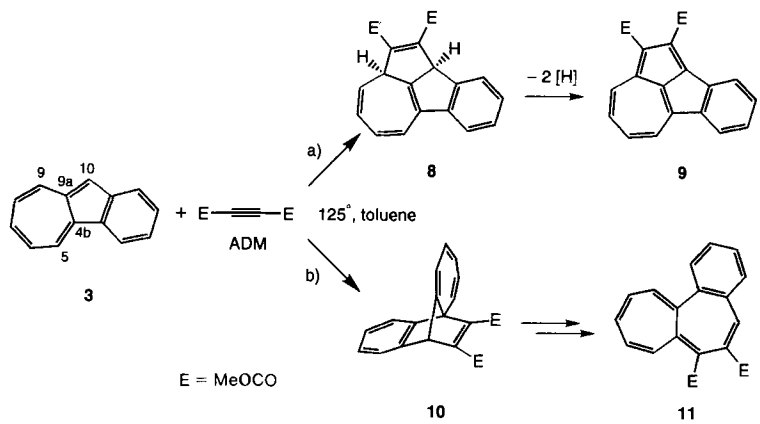

a) 'Heptafulvene' path (*i.e.*, reaction at C(9) and C(10)): *ca.* 1.6%; only **9** can be isolated [29]. b) 'Azulene' path (*i.e.*, reaction at C(4b) and C(10)): *ca.* 98.4%; a mixture of **10** (51.7%) and its thermal rearrangement product **11** (23.4%) is isolated after 40 h. *Ca.* 2% of **3** are also recovered [29]. Similarly, the thermal reaction of the 5,9-diphenyl derivative of **3** and ADM (100°/18 h, MeCN) results in the formation of the 8,12-diphenyl derivative of **11** (83%) and only traces of a rearranged product of the corresponding diphenyl derivative of **8** [30] (*cf.* [26]).

If the heptafulvene substructure is dominating in benz[*a*]azulenes, one would expect to observe the cycloaddition reactivity of heptafulvenes, which results, in the presence of ADM, in a [8 + 2] cycloaddition at the C(1) and C(8) termini (*cf.* [31]). This means that benz[*a*]azulenes would react thermally with ADM to yield benzannelated dimethyl tricyclo[5.4.1.$0^{4,12}$]dodeca-3,5,7(12),8,10-pentaene-2,3-dicarbocylates **8**. These compounds

or their derivatives (*e.g.* **9**), have only been observed as minor products in the thermal cycloaddition chemistry of benz[*a*]azulenes (see *Scheme 2*)[5]).

We thank Prof. *M. Hesse* and his coworkers for mass spectra and Mrs. *J. Kessler* for elemental analyses. The financial support of this work by the *Swiss National Science Foundation* is gratefuly acknowledged. *M. B.* wishes to thank Prof. *W. Thiel* and the *Fonds der Chemischen Industrie* for support. Calculations were performed on *IBM RS/6000* workstations at the *Rechenzentrum der Universität Zürich* and at the *ETH-Zürich* (C4 cluster).

Experimental Part

1. Crystal-Structure Determination[6]). – For each compound, all measurements were conducted at low-temperature on a *Rigaku AFC5R* diffractometer using graphite-monochromated MoK_α radiation ($\lambda = 0.71069$ Å) and a 12-kW rotating anode generator. The intensities were collected using $\omega/2\theta$ scans. Three standard reflections measured every 150 reflections showed negligible variation in intensity. The intensities were corrected for *Lorentz* and polarization effects, but not for absorption. The structures were solved by direct methods using SHELXS86 [32] which revealed the positions of all non-H-atoms. All refinements were carried out on F using full-matrix least-squares procedures, which minimized the function $\Sigma w(|F_o|-|F_c|)^2$, where $w = [\sigma^2(F_o) + (0.005F_o)^2]^{-1}$. The non-H-atoms were refined anisotropically. For 9-phenylbenz[*a*]azulene (**4**), there are two independent molecules in the asymmetric unit. All of the H-atoms were located in a difference electron-density map and were refined isotropically. A correction for secondary extinction was applied for 4-phenylazulene (**5**), all of the H-atoms could be located in a difference electron-density map, but were subsequently fixed in geometrically idealized positions

Table 9. *Crystallographic Data*

	4	**5**
Crystallized from	Hexane	Hexane
Empirical formula	$C_{20}H_{14}$	$C_{16}H_{12}$
Formula weight	254.33	204.27
Crystal color, habit	green, prism	blue, prism
Crystal dimensions [mm]	0.12 × 0.27 × 0.37	0.15 × 0.19 × 0.38
Temp. [K]	173 (1)	173 (1)
Crystal system	triclinic	orthorhombic
Space group	$P\bar{1}$	$Pna2_1$
Z	4	4
Reflections for cell determination	25	18
2θ range for cell determination [°]	37–40	34–38
Unit cell parameters a [Å]	10.994 (1)	7.601 (2)
b [Å]	14.839 (1)	20.785 (3)
c [Å]	9.5524 (9)	7.297 (2)
α [°]	93.326 (9)	90
β [°]	109.360 (8)	90
γ [°]	68.685 (8)	90
V [Å^3]	1366.3 (3)	1152.9 (4)
D_x [g cm^{-3}]	1.236	1.177

[5]) Indeed, the observed benzannelated tricyclo[6.2.2.0^{1,7}]dodeca-2,4,6,9,11-pentaenes **10** also correspond to a formal [8 + 2] cycloaddition of ADM with the heptafulvene substructure in the benz[*a*]azulenes. However, the discussed parent tricycle shows, according to *MM3* calculations, a much higher ΔH_f° value (114 kcal mol^{-1}) than the parent tricycle (ΔH_f° value 83 kcal mol^{-1}) resulting from the [8 + 2] cycloaddition at C(9) and C(10) of the benz[*a*]azulenes, *i.e.*, the latter addition mode should be strongly favored on energetic grounds which should already be expressed in the transition state of the [8 + 2] cycloadditions.

[6]) Crystallographic data (excluding structure factors) for the structures reported in this paper have been deposited with the *Cambridge Crystallographic Data Centre* as supplementary publication No. CCDC-10/1. Copies of the data can be obtained, free of charge, on application to the Director, CCDC, 12 Union Road, Cambridge CB2 1EZ, UK. (fax: +44-(0)1223-336033 or email: teched @ chemcrys.cam.ac.uk).

Table 9 (cont.)

	4	5
$\mu(MoK_\alpha)$ [mm^{-1}]	0.0700	0.0660
$2\theta_{(max)}$ [°]	55	55
Total reflections measured	6601	1887
Symmetry-independent reflections	6277	1629
Reflections used [$I > 2\sigma(I)$]	4059	1116
Parameters refined	474	156
R	0.0472	0.0381
wR	0.0427	0.0309
Goodness of fit	1.508	1.326
Secondary extinction coefficient	8.65×10^{-7}	–
Final Δ_{max}/σ	0.0003	0.0002
$\Delta\rho$ (max; min) [e $Å^{-3}$]	0.22; −0.16	0.16; −0.17

with a C–H distance of 0.95 Å, and only their isotropic temp. factors were allowed to refine. Data collection and refinement parameters are given in *Table 9*. Views of the molecules are shown in *Fig. 2*.

Neutral atom-scattering factors for non-H-atoms were taken from *Maslen*, *Fox*, and *O'Keefe* [33], and the scattering factors for H-atoms were taken from *Stewart*, *Davidson*, and *Simpson* [34]. Anomalous dispersion effects were included in F_{calc} [35]; the values for f' and f'' were those of *Creagh* and *McAuley* [36]. All calculations were performed using the TEXSAN crystallographic software package [37].

2. NMR Measurements. – The NMR spectra were measured on either a *Bruker AMX-600* or *ARX-300* spectrometer at 300 K. For the assignment of H and C signals in $CDCl_3$ and in CD_2Cl_2, selective decoupling and ^{1}H-COSY experiments as well as gradient enhanced HSQC [38] and HMBC [39] experiments were performed. All assignments for benz[*a*]azulene in CD_2Cl_2 were unambiguously confirmed by a proton-detected INEPT-INADEQUATE experiment [11]. The signal assignment in other solvents is based on an evaluation of the coupling pattern in the ^{1}H spectrum and a ^{1}H,^{13}C-correlation experiment (HSQC) for each solvent.

3. Computational Methods. – Geometries have been optimized employing standard methods and 6-31G* basis set [40] (five cartesian d-functions) using the Gaussian 92 program package [41]. Initial geometries have been obtained at the *Hartree-Fock* or self-consistent-field (SCF) level; the nature of the stationary points has been probed by analytical frequency calculations, followed by re-optimizations at the electron-correlated MP2 level and at a gradient-corrected level of density functional theory (DFT) (see *e.g.* [42]), employing the *Becke* 1988 [43] and *Perdew* 1986 [44] exchange and correlation functionals (denoted BP86). MP2/6-31G* atomic charges have been computed employing natural population analysis (NPA) [45].

Chemical shifts have been computed employing the gauge including atomic orbitals (GIAO)-SCF method [46] as implemented [47] in the TURBOMOLE program [48] and a triple-zeta plus polarization basis set (tzp), *i.e.*, *Dunning*'s [49] [5s3p1d] contraction of the *Huzinaga* (9s5p1d) primitive set for C (d-exponent 0.8), and a (5s1p) set contracted to [3s1p] for H [50] (p-exponent 0.8). Various sets of geometries have been employed, and the results are given in the notation 'level of chemical shift calculation // level of geometry optimization'. Benzene has been used as the primary, theoretical reference (with absolute, computed shieldings of 61.1, 55.9, and 58.1 ppm for ^{13}C and 24.8, 24.2, and 24.5 ppm for ^{1}H, employing the SCF/6-31G*, BP86/6-31G* and MP2/6-31G* geometries, respectively), and the results have been converted to the usual δ scale using the experimental chemical shifts of benzene, $\delta(^{13}C) = 128.5$ [51] and $\delta(^1H) = 7.3$ ppm [52].

For *azulene* (**6**) (MP2/6-31G* geometry), ^{13}C chemical shifts have also been computed at the electron-correlated GIAO-MP2 level [18] [19], employing the Aces II program [53] and TZP′ basis, *i.e.*, *Dunning*'s (10s6p1d)/[5s3p1d] contraction [50] for carbon (d-exponent 0.654, six cartesian Gaussians) and the double-zeta (4s)/[2s] contraction for H [49] (absolute, computed C shielding for benzene: 87.8 ppm at GIAO-MP2/TZP′//MP2/6-31G*).

4. Syntheses. – *General*: See [1]. 4.1. *Benz[a]azulene* (**3**): see [1]. 4.1.1. *10-(Phenylsulfonyl)benz[a]azulene* (**2**): see [1]. *Data of* **2**: ^{1}H-NMR (600 MHz, $CDCl_3$)[7]: 9.51 (*d*, $^3J(9,8) = 10.9$, H–C(9)); 8.74 (*d*, $^3J(5,6) = 8.7$, H–C(5));

[7]) We erroneously mistook the assignment of H–C(4) and H–C(5) in [1].

8.58 (*d*, $^3J(1,2) = 8.3$, H–C(1)); 8.36 (*d*, $^3J(4,3) = 7.9$, H–C(4)); 8.05 (*d*, $^3J = 7.64$, 2 H–C(2,6) of $PhSO_2$); 7.77 (*t*, $^3J(2,1) = {}^3J(2,3) = 8.1$, H–C(2)); 7.67 (*t*, $^3J(7,6) = {}^3J(7,8) = 9.8$, H–C(7)); 7.56–7.49 (3*t*, overlapping, 3 H–C(3,8,6)); 7.43 (*t*, $^3J = 7.0$, H–C(4) of $PhSO_2$); 7.39 (*t*, $^3J = 7.7$, 2 H–C(3,5) of $PhSO_2$). ^{13}C-NMR (151 MHz, $CDCl_3$): 143.97 (*s*, C(1) of $PhSO_2$); 141.41 (*s*, C(9a)); 141.25 (*s*, C(4b)); 139.03 (*s*, C(10a)); 137.81 (*d*, C(7)); 134.54 (*d*, C(9)); 132.67 (*d*, C(5)); 132.41 (*d*, C(4) of $PhSO_2$); 130.23 (*d*, double intensity, C(2 and 8)); 129.92 (*s*, C(4a)); 129.28 (*d*, C(6)); 128.86 (*d*, double intensity, C(3 and 5) of $PhSO_2$); 125.81 (*d*, double intensity, C(2 and 6) of $PhSO_2$); 123.22 (*d*, C(3)); 120.87 (*d*, C(4)); 120.48 (*d*, C(1)); 117.61 (*s*, C(10)).

4.1.2. *Data of* **3**: ^{1}H-NMR (600 MHz, CD_2Cl_2): 8.28 (*dd*, $^3J(4,3) = 7.9$, $^4J(4,2) = 0.8$, H–C(4)); 8.23 (*dt*, $^3J(5,6) = 8.3$, $^4J(5,7) = 1.0$, $^5J(5,10) = 1.0$, H–C(5)); 7.86 (*dd*, $^3J(9,8) = 10.9$, $^4J(9,7) = 0.7$, H–C(9)); 7.77 (*d*, $^3J(1,2) = 7.8$, H–C(1)); 7.57 (*td*, $^3J(2,1) = {}^3J(2,3) = 7.6$, $^4J(2,4) = 1.0$, H–C(2)); 7.38 (*td*, $^3J(3,2) = {}^3J(3,4) = 7.6$, $^4J(3,1) = 1.0$, H–C(3)); 7.23 (*s*, H–C(10)); 7.19 (*dd*, $^3J(7,6) = 11.1$, $^3J(7,8) = 8.5$, H–C(7)); 6.96 (*dd*, $^3J(6,7) = 11.1$, $^3J(6,5) = 8.3$, H–C(6)); 6.84 (*dd*, $^3J(8,9) = 10.9$, $^3J(8,7) = 8.5$, H–C(8)). ^{13}C-NMR (151 MHz, CD_2Cl_2): 142.40 (*s*, C(10a)); 140.58 (*s*, C(4b)); 139.20 (*s*, C(9a)); 135.94 (*d*, C(9)); 134.64 (*d*, C(7)); 131.41 (*s*, C(4a)); 128.48 (*d*, C(2)); 127.86 (*d*, C(5)); 125.35 (*d*, C(6)); 123.66 (*d*, C(8)); 121.78 (*d*, C(3)); 120.78 (*d*, C(4)); 120.25 (*d*, C(1)); 116.06 (*d*, C(10)).

4.2. *9-Phenylbenz[a]azulene* (**4**): see [1].

4.3. *9-((*$^2H_5$*)Phenyl)benz[a]azulene* ((D$_5$)-**4**): 4.3.1. *9-((*$^2H_5$*)Phenyl)-10-(phenylsulfonyl)benz[a]azulene:* (D_5)PhLi was prepared by the addition of soln. of (D_5)PhBr (1.0 g, *Armar*, 99%) in Et_2O (15 ml) to excess Li dust (0.3 g, *Alfa*) in Et_2O (10 ml) at 36°. To a soln. of **2** (0.158 g) in THF (3 ml) at −78°, a soln. of (D_5)PhLi in Et_2O was added until the color changed from dark-violet to pale-yellow. To the resulting mixture, MeOH (*ca.* 1 drop) was added and the whole poured onto sat. aq. NH_4Cl. The soln. was extracted with Et_2O. The Et_2O extracts were dried (Na_2SO_4), and the solvent was removed. The residue was dissolved in toluene (5 ml), *o*-chloroanil (0.125 g) added, and the mixture stirred for 16 h at r.t. The brown-yellow suspension was filtered and the precipitate washed with H_2O and then, with Et_2O: (D_5)-**2** (0.132 g; 67%) was obtained as fine black needles. ^{1}H-NMR (600 MHz, $CDCl_3$): 8.77 (*d*, $^3J = 8.6$, H–C(4)); 8.41 (*d*, $^3J = 8.1$, H–C(1)); 8.38 (*d*, $^3J = 8.0$, H–C(5)); 7.74 (*td*, $^3J = 7.1$, $^4J = 1.2$, H–C(2)); 7.60–7.43 (*m*, 4 H–C(3,6,7,8)); 7.40 (*tt*, $^3J = 7$, $^4J = 1.2$, H–C(4) of $PhSO_2$); 7.25 (*d*, $^3J = 7.2$, 2 H–C(2,6) of $PhSO_2$); 7.17 (*t*, $^3J = 7$, 2 H–C(3,5) of $PhSO_2$).

4.3.2. *9-((*$^2H_5$*)Phenyl)benz[a]azulene* ((D$_5$)-**4**): The azulene from *4.3.1* (0.132 g), $Na_2S_2O_4$ (0.088 g), and $NaHCO_3$ (0.10 g) were dissolved in DMF (3 ml), and H_2O (1 ml) was added. The flask was immersed into a pre-heated oil bath at 85–90° and the turbid suspension of brown-green color was stirred. The color of the mixture changed to dark-blue. As soon as the soln. was clear, the mixture was poured into ice/water (50 ml). The resulting green suspension was saturated with NaCl, stirred for 15 min, and the precipitate filtered off. The residue was dissolved in a few ml of CH_2Cl_2, then hexane (10 ml) was added and the soln. concentrated to 3 ml. This soln. was filtered over *Alox* (Act. III) and eluted with hexane: (D_5)-**4** (0.097 g; 73%) was obtained as dark blue needles. R_f (hexane) 0.16. IR (KBr): 3052*m*, 2985*m*, 2304*m*, 1708*w*, 1602*s*, 1576*s*, 1516*m*, 1475*s*, 1447*m*, 1403*m*, 1376*w*, 1361*m*, 1331*m*, 1264*s*, 1234*s*, 1154*m*, 1056*s*, 916*m*, 895*s*, 862*m*, 823*s*, 741*s*, 548*s*, 528*m*. ^{1}H-NMR (600 MHz, $CDCl_3$): 8.43 (*dd*, $^3J(5,6) = 8.3$, $^4J(5,7) = 1.0$, H–C(5)); 8.42 (*dt*, $^3J(4,3) = 7.9$, $^4J(4,2) \approx {}^5J(4,1) \approx 0.9$, H–C(4)); 7.77 (*dt*, $^3J(1,2) = 7.8$, $^4J(1,3) \approx {}^5J(1,4) \approx 0.9$, H–C(1)); 7.65 (*ddd*, $^3J(2,1) = 7.9$, $^3J(2,3) = 7.1$, $^4J(2,4) = 1.0$, H–C(2)); 7.49 (*ddd*, $^3J(3,4) = 7.9$, $^3J(3,2) = 7.1$, $^4J(3,1) = 1.0$, H–C(3)); 7.28 (*ddd*, $^3J(7,6) = 10.9$, $^3J(7,8) = 9.0$, $^4J(7,5) = 1.0$, H–C(7)); 7.09 (br. *s*, H–C(10)); 7.06 (*ddd*, $^3J(6,7) = 10.9$, $^3J(6,5) = 8.3$, $^4J(6,8) = 0.6$, H–C(6)); 6.87 (*dd*, $^3J(8,7) = 9.0$, $^4J(8,6) = 0.5$, H–C(8)). ^{13}C-NMR (151 MHz): 149.07 (*s*, C(9)); 143.63 (*s*, C(1) of C_6D_5); 141.85 (*s*, C(10a)); 141.05 (*s*, C(4b)); 138.54 (*s*, C(9a)); 134.05 (*d*, C(7)); 131.89 (*s*, C(4a)); 128.42 (*d*, C(2)); 128.18 (*d*, C(5)); 128.15 (*t*, ^3J(C,D) = 24, 2 C_m or 2 C_o of C_6D_5); 127.79 (*t*, ^3J(C,D) = 24, 2 C_o or 2 C_m of C_6D_5); 127.28 (*t*, ^3J(C,D) = 24, C_p of C_6D_5); 125.81 (*d*, C(8)); 124.31 (*d*, C(6)); 121.96 (*d*, C(3)); 120.62 (*d*, C(4)); 120.44 (*d*, C(1)); 117.38 (*d*, C(10)). EI-MS: 260 (20), 259 (100, $M^{+\cdot}$), 258 (35), 257 (40), 256 (21).

4.4. *4-Phenylazulene* (**5**). *Azulene* (**6**; 0.434 g, 3.38 mmol) in THF (10 ml) was added to a soln. of PhLi (0.3 ml, 0.48 mmol of a 1.6M soln. in cyclohexane/Et_2O 7:3) at −78° and stirred for 4 min. To the resulting bright-yellow mixture, MeOH (*ca.* 2 drops) was added and the mixture poured into sat. aq. NH_4Cl. The soln. was extracted with Et_2O. The Et_2O extracts were dried (Na_2SO_4), and the solvent was removed. The residue was dissolved in toluene (20 ml), *o*-chloroanil (1.06 g, 4.06 mmol) added, and the mixture was stirred for 15 min at r.t. The soln. was filtered over *Alox* (Act. III). The residue was subjected to CC (hexane) yielding **5** (0.504 g; 73%) as a blue oil. Crystallization from hexane at −30° yielded **5** as fine black needles. M.p. 34–35° ([3]: blue oil). R_f (hexane) 0.3. IR (KBr): 3057*m*, 1588*s*, 1552*s*, 1481*s*, 1443*m*, 1390*m*, 1355*m*, 1213*s*, 990*s*, 923*s*, 835*s*, 762*s*, 700*s*, 648*s*, 475*m*. ^{1}H-NMR (300 MHz, $CDCl_3$): 8.42 (*d*, $^3J(8,7) = 9.4$, H–C(8)); 7.83 (*t*, $^3J(2,1) = J(2,3) = 3.8$, H–C(2)); 7.65–7.57 (*m*, H–C(6), 2 H_o); 7.52–7.44 (*m*, H–C(1), 2 H–C_m, H–C_p); 7.18 (*d*, $^3J(5,6) = 10.4$, H–C(5)); 7.16 (*t* overlapping with H–C(5), $^3J(7,8) = {}^3J(7,6) \approx 9.7$, H–C(7)); 7.13 (br. *d*, overlapping with H–C(5), $^3J(3,2) \approx 3.8$, H–C(3)). ^{13}C-NMR (151

MHz): 150.22 (*s*, C(4)); 143.67 (*s*, C(1) of Ph); 141.03 (*s*, C(8a)); 137.54 (*s*, C(3a)); 137.16 (*d*, C(8)); 136.31 (*d*, double intensity, C(2 and 6)); 129.10 (*d*, double intensity, 2 C_o or 2 C_m of Ph); 128.05 (*d*, double intensity, 2 C_m or 2 C_o of Ph); 127.82 (*d*, C_p of Ph); 125.90 (*d*, C(5)); 121.68 (*d*, C(7)); 119.09 (*d*, C(1)); 118.69 (*d*, C(3)). EI-MS: 205 (16), 204 (100, $M^{+\cdot}$), 203 (89), 202 (50), 200 (7), 101 (6). Anal. calc. for $C_{16}H_{12}$ (204.27): C 94.08, H 5.92; found: C 93.84, H 6.17.

5. *4-((²H$_5$)Phenyl)azulene* ((D$_5$)-**5**). In analogy to **5**, (D$_5$)-**5** (0.241 g; 70%) was obtained as a dark-blue oil. *Data of* (D$_5$)-**5**: R_f (hexane) 0.3. IR: 3025*w*, 2269*w*, 1587*m*, 1555*s*, 1480*s*, 1453*s*, 1436*s*, 1394*m*, 1374*s*, 1356*m*, 1317*s*, 1269*s*, 1254*s*, 1212*m*, 1176*s*, 1066*s*, 1046*s*, 986*m*, 919*m*, 821*m*, 769*s*, 716*s*, 658*s*, 622*s*, 551*m*, 506*m*, 468*m*, 462*m*, 451*s*. ^{1}H-NMR (600 MHz, $CDCl_3$): 8.46 (*d*, $^3J(8,7) = 9.4$, H–C(8)); 7.88 (*t*, $^3J(2,1) = {}^3J(2,3) = 3.8$, H–C(2)); 7.65 (*tdd*, $^3J(6,5) = {}^3J(6,7) = 10.1$, $^6J(6,1) = 1.2$, $^4J(6,8) = 0.6$, H–C(6)); 7.51 (*dd*, $^3J(1,2) = 3.8$, $^6J(1,6) = 1.1$, H–C(1)); 7.22 (*d*, $^3J(5,6) = 10.4$, H–C(5)); 7.20 (*t* overlapping with H–C(5), $^3J(7,8) = {}^3J(7,6) \approx 9.7$, H–C(7)); 7.19 (br. *d*, overlapping with H–C(5), $^3J(3,2) \approx 3.8$, H–C(3)). ^{13}C-NMR (151 MHz): 150.19 (*s*, C(4)); 143.50 (*s*, C(1) of C_6D_5); 141.04 (*s*, C(8a)); 137.55 (*s*, C(3a)); 137.19 (*d*, C(8)); 136.30 (2*d*, C(2 and 6)); 128.70 (*t*, $^3J(C,D) = 24.3$, 2 C_o or 2 C_m of C_6D_5); 127.55 (*t*, $^3J(C,D) = 24.3$, 2 C_m or 2 C_o of C_6D_5); 127.32 (*t*, $^3J(C,D) = 24.6$, C_p of C_6D_5); 125.09 (*d*, C(5)); 121.70 (*d*, C(7)); 119.20 (*d*, C(1)); 118.73 (*d*, C(3)). EI-MS: 210 (15), 209 (100, $M^{+\cdot}$), 208 (51), 207 (68), 206 (31), 205 (10).

REFERENCES

[1] a) A. St. Pfau, Pl. Plattner, *Helv. Chim. Acta* **1936,** *19,* 858; b) D. Sperandio, H.-J. Hansen, *ibid.* **1995,** *78,* 765.
[2] D.-J. Bertelli, P. Crews, *Tetrahedron* **1970,** *26,* 4717.
[3] K. Hafner, H. Weldes, *Liebigs Ann. Chem.* **1957,** *606,* 90.
[4] F. H. Allen, J. E. Davies, J. J. Galloy, O. Johnson, O. Kennard, C. F. Macrae, E. M. Mitchell, G. G. Mitchell, J. M. Smith, D. G. Watson, *J. Chem. Info. Comp. Sci.* **1991,** *31,* 187.
[5] From the October, 1995 version of the Cambridge Structural Database the CSD-Refcodes of the 23 structures are: amazul, azlnpr, azulop, besvaw, buhwoq, buxpal, cibfuo, cimyig, damhee, dizfib, dokzae, farsas, farsew, farsia, hevzaj, hevzen, hevzir, hevzox, hewbam, hiblaf, patlif, styraz, vivcim.
[6] H. L. Ammon, G. L. Wheeler, *Acta Crystallogr., Sect. B* **1978,** *34,* 2043.
[7] W. Simon, G. Naville, H. Sulser, E. Heilbronner, *Helv. Chim. Acta* **1956,** *39,* 1107.
[8] J. Weigelt, G. Otting, *J. Magn. Reson.* **1995,** *113,* 128.
[9] K.-P. Zeller, 'Methoden der organischen Chemie', 4th edn., Georg Thieme Verlag, Stuttgart, 1985, Vol. V/2c, p. 127.
[10] P. Bönzli, M. Neuenschwander, *Helv. Chim. Acta* **1991,** *74,* 225.
[11] W. Koźmiński, D. Sperandio, D. Nanz, *Magn. Reson. Chem.* **1996,** in press.
[12] S. Berger, K. P. Zeller, *J. Org. Chem.* **1984,** *49,* 3725.
[13] S. Grimme, *Chem. Phys. Lett.* **1993,** *201,* 67.
[14] P. M. Kozlowski, G. Rauhut, P. Pulay, *J. Chem. Phys.* **1995,** *103,* 5650.
[15] G. A. Webb, in 'Nuclear Magnetic Shieldings and Molecular Structure', Ed. J. A. Tossell, Kluwer Academic Publ., Dordrecht, 1993.
[16] W. Kutzelnigg, U. Fleischer, M. Schindler, in 'NMR Basic Principles and Progress', Springer Verlag, Berlin, 1990, Vol. 23.
[17] K. Wolinski, J. F. Hinton, P. Pulay, *J. Am. Chem. Soc.* **1990,** *112,* 8251.
[18] J. Gauss, *Chem. Phys. Lett.* **1992,** *191,* 614.
[19] J. Gauss, *J. Chem. Phys.* **1993,** *99,* 3629.
[20] J. Gauss, *Chem. Phys. Lett.* **1994,** *229,* 198.
[21] J. Gauss, J. F. Stanton, *J. Chem. Phys.* **1995,** *102,* 251.
[22] H. J. Tobler, A. Bander, H. H. Günthard, *J. Mol. Spectrosc.* **1965,** *18,* 239.
[23] U. Fleischer, W. Kutzelnigg, P. Lazzeretti, V. Mühlenkamp, *J. Am. Chem. Soc.* **1994,** *116,* 5298.
[24] R. Hollenstein, A. Mooser, M. Neuenschwander, W. v. Philipsborn, *Angew. Chem.* **1974,** *86,* 595.
[25] R. A. Fallahpour, H.-J. Hansen, *Helv. Chim. Acta* **1995,** *78,* 1993.
[26] A. J. Rippert, H.-J. Hansen, *Helv. Chim. Acta* **1993,** *76,* 2906.
[27] R. Hunziker, D. Sperandio, H.-J. Hansen, *Helv. Chim. Acta* **1995,** *78,* 772.
[28] M. Yasunami, T. Sato, M. Yoshifuji, *Tetrahedron Lett.* **1995,** *36,* 103.
[29] J. Guspanová, H.-J. Hansen, unplublished results.
[30] A. Linden, M. Meyer, P. Mohler, A. J. Rippert, H.-J. Hansen, *Helv. Chim. Acta* **1996,** *79,* in preparation.

[31] J. Daub, J. Bindel, P. Seitz, U. Seitz, E. Salbeck, J. Salbeck, J. Bindel, *Chem. Ber.* **1987,** *120,* 1747.
[32] G. M. Sheldrick, SHELXS-86, *Acta Crystallogr., Sect. A* **1990,** *46,* 467.
[33] E. N. Maslen, A. G. Fox, M. A. O'Keefe, in 'International Tables for Crystallography', Ed. A. J. C. Wilson, Kluwer Academic Publishers, Dordrecht, 1992, Vol. C, Table 6.1.1.1, pp. 477–486.
[34] R. F. Stewart, E. R. Davidson, W. T. Simpson, *J. Chem. Phys.* **1965,** *42,* 3175.
[35] J. A. Ibers, W. C. Hamilton, *Acta Crystallogr.* **1964,** *17,* 781.
[36] D. C. Creagh, W. J. McAuley, in 'International Tables for Crystallography', Ed. A. J. C. Wilson, Kluwer Academic Publishers, Dordrecht, 1992, Vol. C, Table 4.2.6.8., p. 219–222.
[37] TEXSAN. Single Crystal Structure Analysis Software, Version 5.0. Molecular Structure Corporation, The Woodlands, Texas, 1989.
[38] G. Bodenhausen, D. J. Ruben, *J. Chem. Phys. Lett.* **1980,** *69,* 185.
[39] A. Bax, M. F. Summers, *J. Am. Chem. Soc.* **1986,** *108,* 2093.
[40] W. Hehre, L. Radom. P. v. R. Schleyer, J. A. Pople, 'Ab Initio Molecular Orbital Theory', Wiley, New York, 1986.
[41] M. J. Frisch, G. W. Trucks, H. B. Schlegel, P. M. W. Gill, B. G. Johnson, M. W. Wong, J. B. Foresman, M. A. Robb, M. Head-Gordon, E. S. Replogle, R. Gomperts, L. Andres, K. Raghavachari, J. S. Binkley, C. Gonzales, R. L. Martin, D. J. Fox, D. J. DeFrees, J. Baker, J. J. P. Stewart, J. A. Pople, Gaussian92/DFT, Pittsburgh PA, 1992.
[42] R. G. Parr, W. Yang, 'Density Functional Theory of Atoms and Molecules', Academic Press, Oxford, 1989.
[43] A. D. Beck, *Phys. Rev. A* **1988,** *38,* 3098.
[44] J. P. Perdew, *Phys. Rev. B* **1986,** *34,* 7046.
[45] A. E. Reed, R. B. Weinstock, F. Weinhold, *J. Chem. Phys.* **1985,** *83,* 735.
[46] R. Ditchfield, *Mol. Phys.* **1974,** *27,* 789.
[47] M. Häser, R. Ahlrichs, H. P. Baron, P. Weiss, H. Horn, *Theor. Chim. Acta* **1992,** *83,* 455.
[48] R. Ahlrichs, M. Bär, M. Häser, H. Horn, M. Kölmel, *Chem. Phys. Lett.* **1989,** *162,* 165.
[49] T. H. Dunning, *J. Chem. Phys.* **1970,** *53,* 2823.
[50] T. H. Dunning, *J. Chem. Phys.* **1971,** *55,* 716.
[51] H. O. Kalinowski, S. Berger, S. Braun, '^{13}C-NMR-Spektroskopie', Georg Thieme Verlag, Stuttgart, 1984.
[52] H. Günther, 'NMR-Spektroskopie', 3rd edn., Georg Thieme Verlag, Stuttgart, 1992.
[53] J. F. Stanton, J. Gauss, J. D. Watts, W. J. Lauderdale, R. J. Bartlett, Quantum Theory Project, University of Florida, Gainesville FL, 1991.